

# A MICROMACHINED KNUDSEN PUMP FOR ON-CHIP VACUUM

Shamus McNamara<sup>1</sup> and Yogesh B. Gianchandani

Department of Electrical Engineering and Computer Science, University of Michigan, Ann Arbor, USA

## ABSTRACT

This paper describes a single-chip micromachined implementation of a Knudsen pump – a type of vacuum pump that works by the principle of thermal transpiration, has no moving parts, and consequently offers high reliability. A 6-mask process was used to fabricate the pump from a glass substrate and a silicon wafer. A single stage pump and two integrated pressure sensors occupy 1.5 mm X 2 mm. Measurements show that this device can evacuate a cavity to 0.46 atm while operating at atmospheric pressure and using 80 mW input power. Temperature measurements show thermal isolation on the order of  $10^4$  K/W between the polysilicon heater used to operate the pump and the rest of the device.

## I. INTRODUCTION

Only a few types of vacuum pump scale well to small dimensions because the amount of gas back-streaming per unit volume of gas pumped increases as the surface to volume ratio increases. Most vacuum pumps have complicated machinery that does not scale well to microfabrication by planar techniques. A micromachined vacuum pump that has been successfully demonstrated is the getter pump [1], which has no moving parts and relies on the principle of capturing the gas. While effective for maintaining vacuum, getter pumps are less suitable for instruments that sample gases. Thermal molecular pumps can serve this purpose. They are also well-suited for miniaturization because efficiency improves with surface to volume ratio, and they have no valves that must seal.

There are three types of thermal molecular pumps [2]: the Knudsen pump [3], accommodation pump [4], and the thermomolecular pump [5]. The accommodation pump works by taking advantage of the differences in the tangential momentum accommodation coefficient (TMAC) for gases at different temperatures. Although the compression ratio is small (less than 1.1), this pump has no theoretical lower pressure bound. The TMAC depends upon the surface roughness, making the performance of an accommodation pump more variable than for a Knudsen pump. The thermomolecular pump takes advantage of the fact that some materials, when heated, violate the cosine scattering law. This requires special surface conditions that cannot easily be maintained. The Knudsen pump (Fig. 1a) was chosen because it provides the highest compression ratio and its performance is independent of the material surface conditions.

Invented almost a century ago [3], the Knudsen pump was long regarded as a relatively inefficient option for achieving high vacuum [6], despite its attractive feature of

no moving parts. In theory, the Knudsen pump has many potential advantages, such as high reliability, no hydrocarbon backstreaming, and the ability to efficiently pump light gases, such as hydrogen and helium, which many types of pumps do not pump well. A barrier to acceptance has been that sub-micron feature sizes are required for the pump to operate at atmospheric pressure. The evolution of micromachining technology has rekindled interest [2], leading to simulation efforts [7,8], and a partially micromachined implementation achieving a best-case pressure drop of 11.5 Torr using helium [9,10].

Although micromachined gas pumps have many potential uses, there has been very little reported in the literature on their development. They may be used to create a high pressure (compressors), create a low pressure (vacuum pumps), or transport gases with no substantial change in pressure. Potential applications for these devices include driving gases for gas chromatography, spectroscopy [11], and  $\mu$ -plasmas [12,13]; pneumatic pumping of liquids for spectroscopy [14]; or to maintain vacuum on-chip without requiring hermetic packaging for vacuum encapsulated applications.

This paper describes a fully micromachined implementation of a Knudsen pump. The first section will describe the theory of operation of a Knudsen pump, including the expected performance and limitations imposed by geometry. The next section describes the design and fabrication sequence of a single-stage Knudsen pump that occupies an area of only 1.5 mm X 2 mm. Finally, measurement results are presented that show that a single

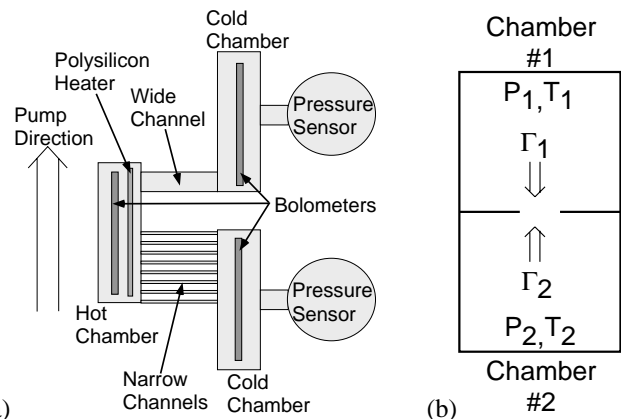


Fig. 1: (a) Layout of a single stage Knudsen pump showing two cold chambers, one hot chamber, the wide channel and parallel narrow channels. (b) Geometry for calculating the equation for thermal transpiration. Two chambers at different temperatures are separated by an ideal aperture, through which a flux of gas molecules flows from either side.

<sup>1</sup> Address: 1301 Beal Ave., Ann Arbor, MI 48109-2122, USA; Tel: (734) 647-0325; Fax: (734) 763-9324; E-mail: shamusm@eecs.umich.edu

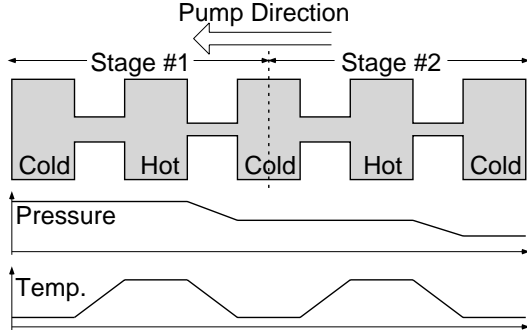


Fig. 2: A two-stage Knudsen pump. At the bottom of the figure is a plot of the temperature and pressure at every stage.

stage pump is capable of generating a pressure of 0.46 atm in a microcavity while maintaining good thermal isolation.

## II. KNUDSEN PUMP THEORY

The Knudsen pump relies on the physical principle of thermal transpiration for its operation. Thermal transpiration gives the following relationship between two adjacent volumes of gas maintained at differing temperatures in the free molecular flow regime (Fig. 1b):

$$\frac{P_1}{P_2} = \sqrt{\frac{T_1}{T_2}} \quad (1)$$

This equation is obtained by equating the flux of gas molecules passing between the chambers. The necessary equations are:

$$\Gamma = \frac{n v_{ave}}{4}; \quad P = nkT; \quad v_{ave} = \left( \frac{8kT}{\pi M} \right)^{1/2} \quad (2)$$

where  $\Gamma$  is the flux of gas molecules going through the aperture,  $v_{ave}$  is the average velocity of the gas molecules,  $n$  is the gas number density,  $P$  is pressure,  $k$  is Boltzmann's constant,  $T$  is temperature, and  $M$  is the mass of a gas molecule. When the gas is in the viscous flow regime, a temperature difference does not create a pressure difference between the chambers.

In practice, the Knudsen pump (Fig. 2) is realized by replacing the ideal aperture with a channel. The pump creates a pressure increase from a cold region to a hot region through a very narrow channel in which the gas is in the free molecular flow regime. Then a wide channel is used to transport the gas from the hot region to a second cold region. The wide channel must ensure that the gas is in the viscous flow regime to avoid thermal transpiration (and hence pumping) in the reverse direction. The attainable pressure ( $P_{vac}$ ) as a function of hot stage temperature ( $T_h$ ), cold stage temperature ( $T_c$ ), the outlet pressure ( $P_{outlet}$ ), and the number of stages ( $s$ ) is:

$$P_{vac} = P_{outlet} \left( \frac{T_c}{T_h} \right)^{s/2} \quad (3)$$

The final pressure distribution is a function of temperature only! Figure 3 shows the expected performance for a single stage and a 3 stage Knudsen pump as predicted by eqn (3). A long channel will reduce the thermal gradient along the channel and hence minimize power consumption, but a short

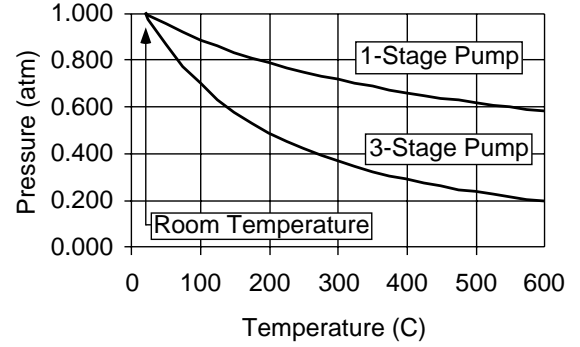


Fig. 3: The theoretical cavity pressure using a single stage and a 3-stage Knudsen pump as a function of the hot chamber temperature.

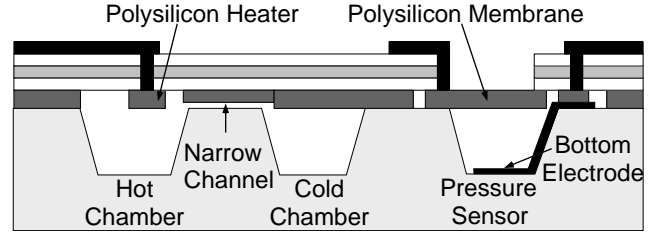


Fig. 4: Cross-section of the Knudsen pump, including hot and cold chambers connected by a narrow channel, and a capacitive pressure sensor used to measure the pump performance.

channel will have a high gas conductance and hence higher flow rates.

The channels in the Knudsen pump must operate in the proper flow regime, which is described by the Knudsen number. The Knudsen number is defined as  $Kn = \lambda / l$ , where  $\lambda$  is the mean free path of the gas and  $l$  is the hydraulic diameter of the channel. Ideally, the narrow channels must have a hydraulic diameter less than 1/10 of the mean free path of the gas (free molecular flow regime,  $Kn > 10$ ) and the wide channels must have a hydraulic diameter greater than 20 times the mean free path of the gas (viscous flow regime,  $Kn < 0.05$ ). However, both types of channels may be operated in the transition flow regime ( $0.05 < Kn < 10$ ) with a possible loss of compression. The maximum operating pressure is determined by the hydraulic diameter of the narrow channels. The smaller the narrow channels, the higher the operating pressure. The lowest attainable pressure is determined by the hydraulic diameter of the wide channels. The larger the wide channels, the lower the attainable pressure. The maximum height of the narrow channels is 6 nm if operation in the free molecular flow regime is to be achieved because the mean free path of air is approximately 60 nm at STP. This small dimension makes it more convenient to design a Knudsen pump that operates in the transition flow regime at its input stage for atmospheric operation.

## III. EXPERIMENTAL DEVICE

Figure 4 shows a cross-section of a hot chamber, a cold chamber, an attached pressure sensor, and identifies their structural layers. The hot chamber is heated with a suspended polysilicon heater located near the narrow channels. The polysilicon heater is suspended on a thin dielectric membrane in order to minimize heat flow from the

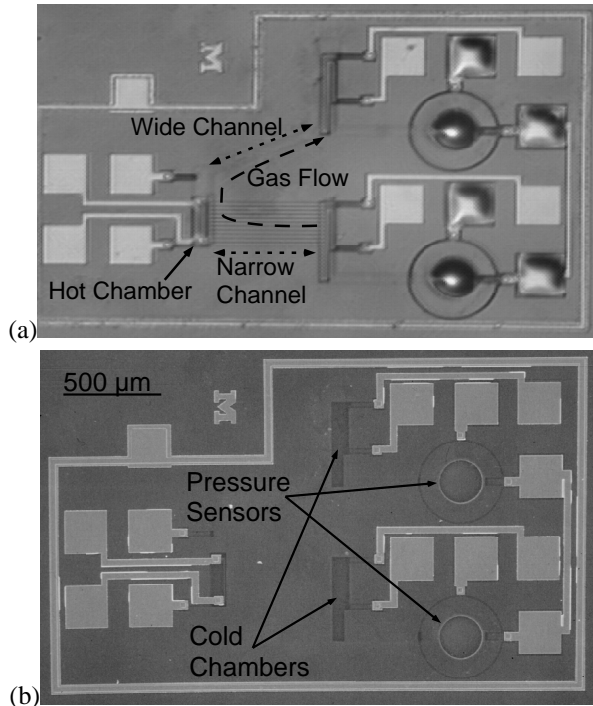


**Fig. 5:** (a, upper) Optical micrograph and (b, lower) SEM of a single stage pump. The pump is sealed, causing the pressure sensor membranes to deflect in the photograph because of the ambient pressure.

heater to the substrate. The cold chambers are passively maintained at room temperature. A glass substrate is used to provide thermal insulation and, thereby, improve the energy efficiency. A long channel length is used to provide good thermal isolation between the hot and cold chambers. Finally, in a multiple stage pump, the hot chambers are all adjacent to each other.

The wide channels are  $10\ \mu\text{m}$  deep and  $30\ \mu\text{m}$  wide. This ensures that the gas flow is in the viscous regime for pressures down to 300 Torr with a hot chamber temperature of  $600\ ^\circ\text{C}$ . The narrow channels are  $10\ \mu\text{m}$  wide and  $100\ \text{nm}$  deep. The mean free path of air at atmospheric pressure and room temperature is  $60\ \text{nm}$ , so the narrow channels correspond to a Knudsen number of 0.6, which is in the transition regime, not the free molecular gas regime. There are many narrow channels in parallel to increase the gas conductance.

Thin film bolometers are located on the bottom every chamber (Fig. 1a). These bolometers are present to provide data on the temperature distribution on the chip, allowing the thermal isolation to be measured.

A capacitive pressure sensor is located adjacent to every cold chamber, as far as possible from the hot chamber to avoid thermal effects. A cross-section of a pressure sensor may be seen in Fig. 4. The top electrode is a  $1\ \mu\text{m}$  thick,  $200\ \mu\text{m}$  diameter polysilicon membrane and the bottom titanium electrode is located at the bottom of a  $10\ \mu\text{m}$  recess in the glass.

#### IV. FABRICATION

A six-mask fabrication process is used to co-fabricate the Knudsen pump and capacitive pressure sensors [15]. A

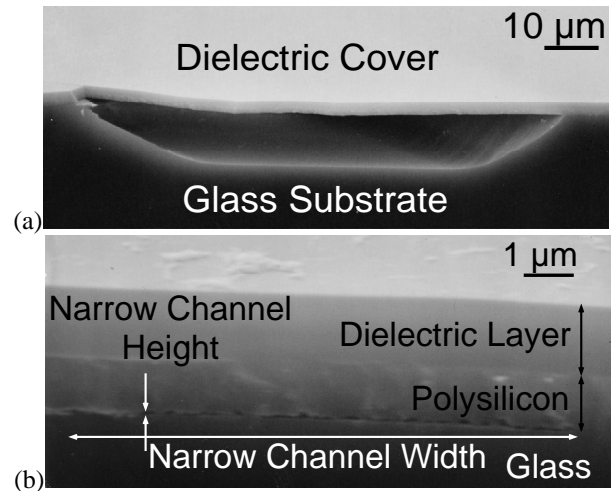


**Fig. 6:** SEM of cross-section of (a, upper) a wide channel  $10\ \mu\text{m}$  deep and (b, lower) a narrow channel only  $100\ \text{nm}$  in height.

Borofloat® glass wafer is etched  $10\ \mu\text{m}$  deep to define the hot and cold chambers, the capacitive pressure sensor cavity, and the wide channels. Titanium is deposited and patterned to define the bolometers and bottom electrode of the capacitive pressure sensor. Separately, a bare silicon wafer is coated with  $\text{SiO}_2$ ,  $\text{Si}_3\text{N}_4$ ,  $\text{SiO}_2$ , and  $100\ \text{nm}$  thick polysilicon. The polysilicon is patterned to define areas for lead transfer and to open narrow channels. An additional  $900\ \text{nm}$  of polysilicon is deposited and the full  $1\ \mu\text{m}$ -thick polysilicon is patterned to isolate regions defining the heater, the top electrode of the capacitive pressure sensor, and to define areas for lead transfer. The glass and silicon wafers are anodically bonded and the entire silicon wafer is dissolved, leaving cavities sealed with dielectric/polysilicon diaphragms. Electrical vias are etched in the dielectric layer and titanium is deposited and patterned to define the top metal and bonding pads (see Fig. 4).

#### V. MEASUREMENT RESULTS

Figure 5 shows an optical micrograph and an SEM image of the same single-stage fabricated device before an outlet is formed for the pump. At this time, the interior of the Knudsen pump is sealed under vacuum. The optical micrograph shows that the pressure sensors are deflected due to the ambient pressure, but the SEM image has flat pressure sensors due to the vacuum ambient. Figure 6 shows SEM images of the channel cross-sections. The wide channel is etched  $10\ \mu\text{m}$  into the glass and has a dielectric cover. The narrow channel is  $10\ \mu\text{m}$  wide but only  $100\ \text{nm}$  high. The figure shows that the polysilicon did not bond to the glass along the narrow channel despite the very small gap.

Figure 7 shows the pressure sensor in device A, a single stage device operated at atmospheric ambient, with power off (Fig. 7a) and with the power on (Fig. 7b). The change in capacitance is  $2.6\ \text{fF}$ , which corresponds to a cavity pressure of  $0.46\ \text{atm}$ . (ANSYS® was used to predict the performance of the pressure sensor including the measured stress of the materials, non-linear effects, and stress-stiffening effects.) Figure 8 shows the response of the pressure sensor in another single stage device, B, as a function of input power.

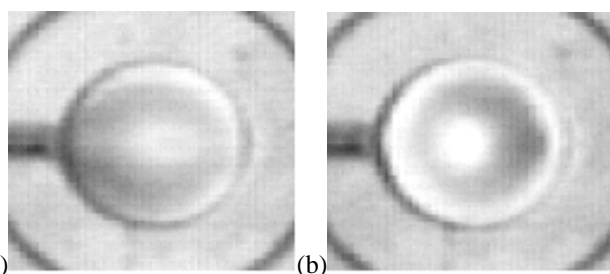


Fig. 7: Picture of a 200  $\mu\text{m}$  diameter pressure sensor (a, left) not deflected and (b, right) deflected when the pump was turned on. The measured capacitance change is 2.6 fF, corresponding to a cavity pressure of 0.46 atm (Device A).

It shows a linear relationship between the applied power and the pressure change. The measured pressure changes range from 0.4-5 Torr/mW for the devices.

The thermal isolation achieved by the Knudsen pump was measured. For device A to obtain a cavity pressure of 0.46 atm, the calculated temperature from eqn. (3) is 1100  $^{\circ}\text{C}$ . At a power dissipation of 80 mW, this corresponds to a thermal resistance of  $1.4 \times 10^4$  K/W, which agrees well with measurements reported in [15]. Using embedded bolometers, the bottom of the hot chamber is measured to rise by  $\approx 10^{\circ}\text{C}$  with 30 mW of power to the polysilicon heater on the diaphragm above it, and a neighboring cold chamber rises less than  $1^{\circ}\text{C}$ . These thermal measurements prove two things: (i) the pressure sensors, being even further away from the heaters, remain at room temperature and therefore do not need to be compensated for temperature; (ii) the pump should experience no loss of performance due to undesired heating of the cold chamber.

## VI. CONCLUSIONS

The single-chip Knudsen pump presented in this paper is the smallest one reported to date, and it is only the second reported Knudsen pump capable of operating at atmospheric pressure. A single stage pump and two integrated capacitive pressure sensors occupy an area 1.5 mm  $\times$  2 mm. The pressure in a microcavity is 0.46 atm at 80 mW of input power. Multiple stages may be cascaded in series to create a pump with a lower ultimate pressure.

Atmospheric operation is made possible by taking advantage of the small feature sizes achievable in microfabrication. Only polysilicon, Si-dielectric materials, metal, and glass are needed, making the 6-mask process silicon IC-compatible. Bolometers are located in the microcavities to verify the temperature distribution on the chip. The temperature of the glass substrate under the polysilicon heaters rose by less than  $10^{\circ}\text{C}$ , and the temperature of the cold chambers rose by less than  $1^{\circ}\text{C}$ , showing excellent thermal isolation.

Although the Knudsen pump was used to evacuate a cavity in this effort, the larger goal was the demonstration of the concept. It may be used for gas sampling applications, pneumatic actuation, and vacuum encapsulation.

## ACKNOWLEDGEMENTS

This work was supported in part by the Engineering Research Centers Program of the National Science Foundation under Award

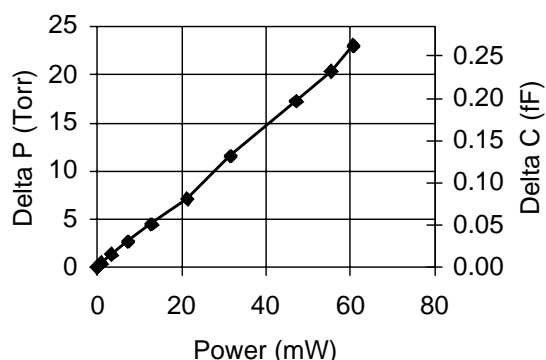


Fig. 8: Measured pressure change with increasing pump power for Device B.

Number EEC-9986866. The facilities used for this research include the Solid-State Electronics Laboratory (SSEL) at the University of Michigan.

## REFERENCES

- [1] P.P.L. Chang-Chien, K.D. Wise, "Wafer-Level Packaging Using Localized Mass Deposition," *Transducers'01*, pp. 182-5, 2001
- [2] J.P. Hobson, D.B. Salzman, "Review of pumping by thermal molecular pressure," *Journal of Vacuum Science & Technology A*, 18(4), pp. 1758, 2000
- [3] M. Knudsen, *Annals Der Physik*, 31, pp. 205, 1910
- [4] J.P. Hobson, "Accommodation Pumping - A New Principle," *J. Vac. Sci. and Tech.*, 7(2), pp. 351-7, 1970
- [5] D. H. Tracey, "Thermomolecular pumping effect," *Journal of Physics E: Scientific Instruments*, 7, pp. 533, 1974
- [6] D.J. Turner, "A mathematical analysis of a thermal transpiration vacuum pump," *Vacuum* 16(8), pp. 413, 1966
- [7] C.C. Wong, M.L. Hudson, D.L. Potter, T.J. Bartel, "Gas Transport by Thermal Transpiration in Micro-Channels - A Numerical Study," 1998 ASME MEMS Conference, DSC-Vol. 66, pp. 223, Anaheim, California, 1998
- [8] R.M. Young, "Analysis of a micromachine based vacuum pump on a chip actuated by the thermal transpiration effect," *Journal Vacuum Science and Technology B*, 17(2), pp. 280, 1999
- [9] S.E. Vargo, E.P. Muntz, G.R. Shiflett, "Knudsen compressor as a micro- and macroscale vacuum pump without moving parts or fluids," *Journal Vacuum Science and Technology A*, 17(4), pp. 2308, 1999
- [10] S.E. Vargo, E.P. Muntz, "Initial Results From the First MEMS Fabricated Thermal Transpiration-Driven Vacuum Pump," *Rarefied Gas Dynamics: 22nd Intl. Symp.*, pp. 502-509, 2001
- [11] R.A. Miller, E.G. Nazarov, G.A. Eiceman, and A.T. King, "A MEMS radio-frequency ion mobility spectrometer for chemical vapor detection," *Sens. Actuators A, Phys.*, 91, pp.301-12, 2001
- [12] C. Wilson and Y.B. Gianchandani, "Silicon micro-machining using in-situ DC microplasmas," *IEEE J. Microelectromechanical Sys.*, 10(1), pp.50-4, 2001
- [13] F. Iza and J. Hopwood, "Influence of operating frequency and coupling coefficient on the efficiency of microfabricated inductively coupled plasma sources," *Plasma Sources Science and Technology*, 11, pp 1-7, 2002
- [14] C. Wilson and Y.B. Gianchandani, "LED-SpEC: Spectroscopic detection of contaminants using glow discharges from liquid microelectrodes," *IEEE MEMS'02*, pp. 248-51, 2002
- [15] S. McNamara and Y.B. Gianchandani, "A Fabrication Process with High Thermal Isolation and Vacuum Sealed Lead Transfer for Gas Reactors and Sampling Microsystems," *IEEE MEMS'03*, pp. 646-9, 2003